ELSEVIER

Polymer 43 (2002) 2671–2676

polymer

www.elsevier.com/locate/polymer

Estimation of crystallinity of isotactic polypropylene using Raman spectroscopy

A.S. Nielsen[a], D.N. Batchelder[b], R. Pyrz[a,*]

[a]*Institute of Mechanical Engineering, Aalborg University, Pontoppidanstraede 101, 9220 Aalborg East, Denmark*
[b]*Department of Physics and Astronomy, University of Leeds, LS2 9JT Leeds, UK*

Received 13 August 2001; accepted 28 December 2001

Abstract

A method to estimate the degree of crystallinity in isotactic polypropylene has been developed. The method is based on integrated intensities of the Raman bands at 808 and 841 cm^{-1}. From the observation of correlation splitting, Raman bands related to different conformational states were identified. This analysis indicates the existence of three different conformational states. The 808 cm^{-1} band was assigned to helical chains within crystals. The 840 cm^{-1} band was shown to be composed of a band at 840 cm^{-1}, assigned to shorter chains in helical conformation, and a broader band at 830 cm^{-1} assigned to chains in non-helical conformation. In order to establish a quantitative relation between Raman scattering intensity and crystallinity samples subjected to different cooling rates and crystallisation temperatures were analysed. These results correlate well with those of differential scanning calorimetry.

Keywords: Polypropylene; Crystallinity; Raman spectroscopy

1. Introduction

The microstructure of a semicrystalline polymer is heterogeneous consisting of crystalline and non-crystalline regions. The heterogeneity of the microstructure comes from the different molecular structure of the amorphous and crystalline regions. In the amorphous regions, chains are randomly coiled whereas in the crystals they are arranged in a three-dimensional lattice. Due to this heterogeneity, properties must be highly influenced by the degree of crystallinity [1–10]. The degree of crystallinity for a semicrystalline polymer is highly dependent on the thermal history, tacticity and deformation [11–14]. Thus in the polymer processing technology it is relevant to consider means of characterising the microstructure in order to evaluate the effect of various processing parameters.

There are a wide range methods available for the characterisation of polymers. Differential scanning calorimetry (dsc), density measurements and X-ray scattering provide quantitative measures of the degree of crystallinity. However, determination of crystallinity from these methods is based on the assumption of a two-phase structure which may indeed not be the case. Previous studies on semicrystalline polymers using vibrational spectroscopy have shown the existence of an intermediate non-crystalline phase associated with the lamella structure [15–18]. Raman and Infrared vibrational spectroscopies probe the conformational states of the polymer chains. Thus differences in the vibrational spectrum of chains in crystals with a unique, regular helical conformation and chains in non-crystalline regions with conformational irregularities or non-helical conformation must be expected [17,18,20,21]. Consequently it may be possible to identify bands of the vibrational spectrum of the polymer related to chains in specific 'phases'. Raman spectroscopy has been widely used for studying regularity and local structures in polymers including polyethylene terephthalate (PET), polyethylene (PE), polystyrene, polyetheretherketone and polytetraflourethylene (PTFE) [13,14,16–18,20–29]. The drawback of the Raman method is the difficulty of performing quantitative measurements as the Raman spectrum is usually only sensitive to chain conformation and insensitive to the lateral order of the crystalline phase. This paper describes a systematic experimental study into the relation between Raman scattering and microstructure of isotactic polypropylene (i-PP). The purpose of this study is to derive a quantitative relation between Raman scattering and crystallinity.

* Corresponding author. Fax: +45-9815-9305.
E-mail address: rp@ime.auc.dk (R. Pyrz).

0032-3861/02/$ - see front matter
PII: S0032-3861(02)00053-8

2. Experimental study of conformational states in i-PP

In order to determine the crystallinity, of the polymer it is necessary to identify Raman bands related to scatters within the crystalline as well as non-crystalline domains. Raman scattering reflects the conformation of the polymer chains as this determines the vibrational state. Chains in amorphous regions have isomeric defects and are not capable of forming regular helices necessary for crystallisation. For a non-helical chain there is no coupling between molecular vibrations in neighbouring repeat units as their relative motions cancel out along the chain due to the lack of translational symmetry. Each repeat unit may then be regarded as an isolated molecule in its own environment and the Raman spectrum reflects the fundamental modes of the chemical repeat units. If chains are regular, they form helices and the fundamental vibrations of each repeat unit become correlated when they vibrate in phase as a result of the translational symmetry of the chain. In this case, the fundamental frequencies split into modes characteristic of the chain and these are referred to as regularity modes. Correlation splitting characteristic for the crystal may also take place if inter-chain interactions are significant and these are referred to as crystal modes. However, usually intra-chain forces are much stronger than inter-chain forces and correlation splitting characteristic of the crystal is weak or absent. If a fundamental vibration is highly localised it is not affected by the chain conformation and is referred to as a group frequency.

From a comparison of Raman spectra in the melt (amorphous) and solid (partly crystalline) state correlation splitting associated with chain conformation and crystallisation can be observed. Figs. 1 and 2 show the Raman spectrum in melt (amorphous) and solid (partially crystalline) state. The Raman scattering was produced by a 633 nm line of a HeNe laser and spectra were recorded using a Renishaw Raman microscope with a 10× objective.

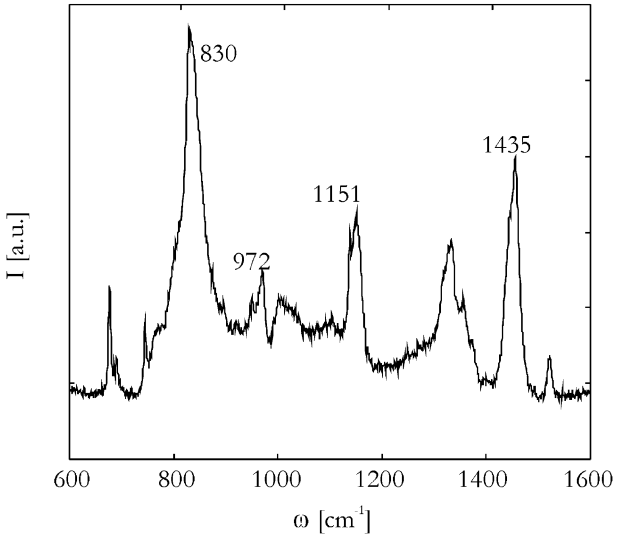

Fig. 1. Raman spectrum of i-PP in melt (amorphous) state.

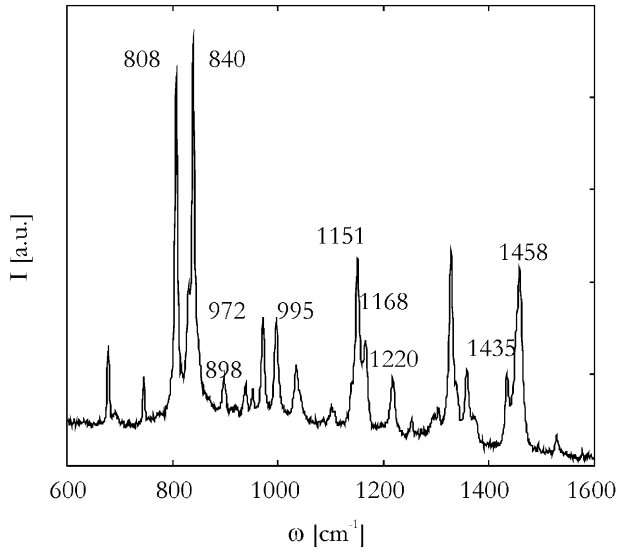

Fig. 2. Raman spectrum of i-PP in solid (partially crystalline) state.

Peaks that disappear completely in the melt are those that can be assigned to the helical chain conformation or crystal unit cell. Peaks that do not disappear are those that can be assigned to group frequencies or helical chains where the intra-molecular coupling between adjacent chemical repeat units is weak. The vibrational assignments of the Raman peaks of i-PP are given in Table 1. Fig. 3 shows some characteristic frequencies of chemical groups present in the chemical repeat unit of i-PP.

Raman bands are observed in the melt state at 830, 972, 1151 and 1435 cm^{-1}. The bands at 972, 1151 and 1435 cm^{-1} are present in the melt as well as in the partially crystalline state. This indicates that these bands are due to fundamental frequencies of the chemical repeat unit or due to localised vibrations within short helical chain segments in the melt (group frequencies). The broadening of the bands in the melt is due to the increasing disorder in the environment of the individual chains upon melting [28]. The 1151 cm^{-1} band has been observed in both isotactic and syndiotactic PP and is thus not specific for the chain conformation

Table 1
Vibrational assignment for Raman bands of i-PP (δ = bending, r = rocking, ν = stretching, t = twisting, w = wagging). From Ref. [31]

ω (cm^{-1})	Vibrational assignment
808	$r(CH_2)$, ν(C–C)
841	$r(CH_2)$
972	$r(CH_3)$, ν(C–C)
998	$r(CH_3)$
1151	ν(C–C), δ(CH)
1168	ν(C–C), $r(CH_3)$, w(C–C)
1220	$t(CH_2)$, w(CH), ν(C–C)
1435	$\delta(CH_2)$
1458	$\delta(CH_2)$

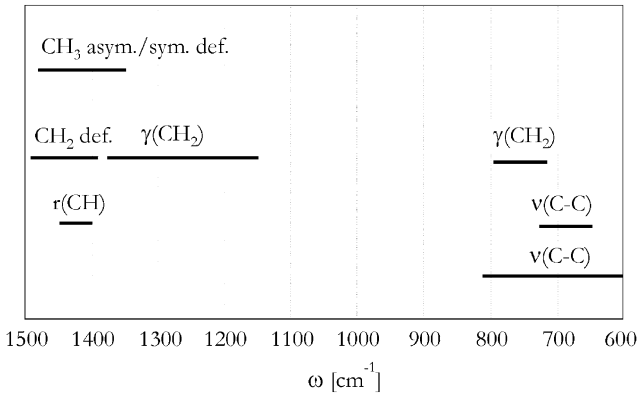

Fig. 3. Characteristic group frequencies.

(group frequency) [29]. The band at 1435 cm^{-1} corresponds well to a group frequency assigned to the CH_2 group deformation, Fig. 3. The 972 cm^{-1} band has been assigned to the symmetry of the 3_1 helical structure [30]. However, the potential energy distribution for this band indicates that the vibrations are highly localised in the CH_3 group [32]. Thus, the appearance of this band is only weakly affected by neighbouring units as intra-chain interactions primarily are accommodated through modes involving the backbone. This explains its appearance in the melt state. The broad asymmetric band observed at approximately 830 cm^{-1} apparently splits into two bands at 808 and 840 cm^{-1} upon crystallisation. This indicates that the 830 cm^{-1} band is a fundamental frequency of the chemical repeat unit that is altered by the symmetry of the helical chain conformation due to inter-molecular coupling between adjacent groups.

Based on normal mode calculations it has been shown that the 808, 840, 898, 972, 995, 1168 and 1220 cm^{-1} bands in the solid state are associated with the helical chain structure [31,32]. The 808, 840 and 1168 cm^{-1} bands come from correlation splittings of the 830 and 1151 cm^{-1} bands. Crystal splitting due to inter-chain interactions in the unit cell has been observed below −196 °C for the 808 and 898 cm^{-1} bands and some other lower frequency bands [33,34]. Although these splittings are very weak they do indicate that these particular regularity

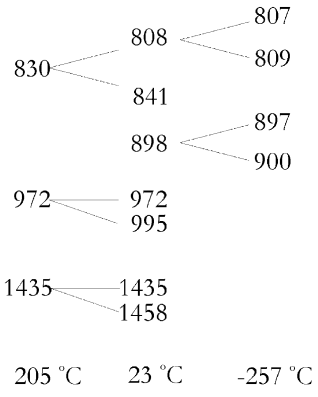

Fig. 4. Raman band splittings of i-PP (cm^{-1}).

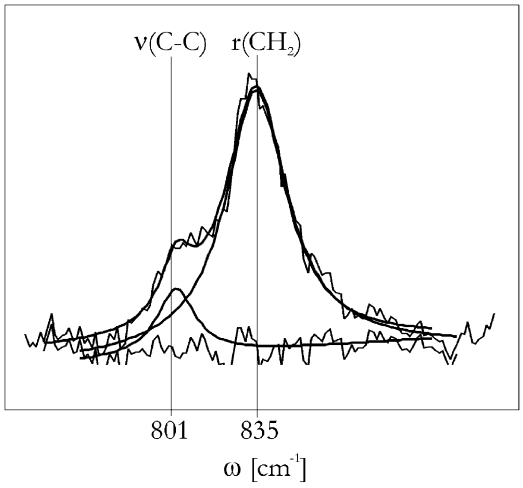

Fig. 5. Lorentzian–Gaussian fit to 808–840 cm^{-1} spectral region in melt. Indication of fundamental group modes.

bands are related to helical chains within the crystals. Fig. 4 summarises the observed splittings in the present study and Ref. [33].

From the earlier analysis, it is seen that significant spectral changes take place during crystallisation. The Raman spectrum is mainly sensitive to the conformational order/disorder (regularity) along the chain length and less sensitive to lateral order in the crystal unit cell. However, as regularity is a necessary condition for crystallisation, the assignment of Raman bands to the specific 'phases' of the microstructure may be accomplished based on the regularity of the chains. Specifically, short helical segments which exhibit isomeric defects as well as chains in a non-helical conformation will be present in non-crystalline regions, whereas the highly regular chains will primarily be present in the crystals.

In order to analyse the Raman scattering quantitatively, the spectrum was fitted to Lorentzian–Gaussian functions. From Fig. 5 it can be seen that the 830 cm^{-1} peak can be fitted to two bands at 801 and 835 cm^{-1} which probably correspond to the ν(C–C) and $r(CH_3)$ fundamental modes. As the polymer solidifies the 830 cm^{-1} band splits into bands at 808 and 840 cm^{-1}. These bands are characteristic of the helical conformation and arise from similar molecular groups as the 830 cm^{-1} band. Thus the 830 cm^{-1} band must be related to chains in non-helical conformation and this spectral region of the melt also resembles that of atactic PP.

Figs. 6 and 7 shows the spectral analysis in the solid state fitted with two and three peaks, respectively. From this analysis it is evident that the 808–840 cm^{-1} spectral region in the solid state is composed of three separate peaks located at 808, 830 and 840 cm^{-1}. The presence of the 830 cm^{-1} band also in the partially crystalline state indicates the presence of atactic chains. The 808 cm^{-1} band must be related to helical chains in the crystal region due to the occurrence of crystal splitting. The 840 cm^{-1} band has been assigned to helical chains were the *trans–gauche*

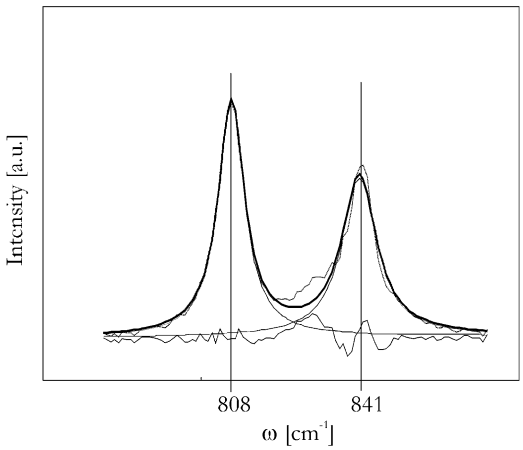

Fig. 6. Lorentzian–Gaussian fit to 808–840 cm^{-1} spectral region. Two peaks.

(*tg*) conformation has been disrupted [29,35]. Comparing the potential energy distribution (PED) on specific modes for the 808 and 840 cm^{-1} band it is seen that the 808 cm^{-1} band is related to $r(CH_3)$ and backbone stretching ν(C–C) whereas the 840 cm^{-1} band is primarily assigned to the $r(CH_3)$ modes. Ize-Iyamu [36] found an increase in the intensity ratio I_{840}/I_{808} with increasing kinking in the *tg* chain conformation. When isomeric defects are introduced in the *tg* conformation, the C–C coupling is partly lost and the main contribution to PED comes from the side-group mode $r(CH_3)$. This causes a shift of Raman band from 808 to 840 cm^{-1} and supports the conclusion that the 840 cm^{-1} is due to helical chains with isomeric defects.

3. Quantitative analysis

In order to establish a quantitative relation between the Raman scattering and crystallinity, samples of different crystallinities were prepared. Thin films of i-PP were melted

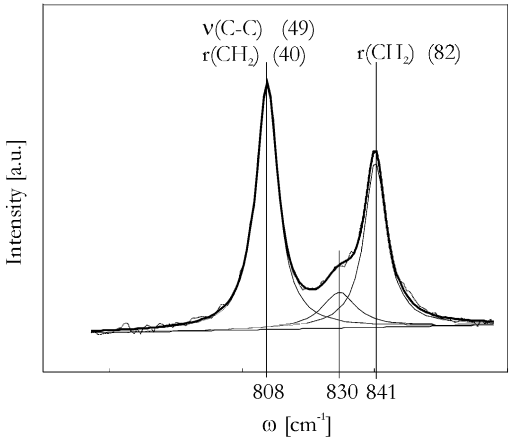

Fig. 7. Lorentzian–Gaussian fit to 808–840 cm^{-1} spectral region. Three peaks. Note the improvement in the residual. Indication of potential energy contribution (%) from group modes.

Table 2
Sample preparation and crystallinity determined by dsc

Sample	Thermal history	χ_c (dsc)
1	Quenched	47.1 ± 0.8
2	Quenched + annealed at 100 °C, 10 min	48.9 ± 6.2
3	Quenched + annealed at 155 °C, 10 min	60.1 ± 4.3
4	Quenched + annealed at 155 °C, 60 min	60.7 ± 2.5
5	Constant cooling rate 130 °C/min	48.8 ± 2.7
6	Constant cooling rate 25 °C/min	50.4 ± 1.5
7	Constant cooling rate 10 °C/min	50.6 ± 1.0
8	Constant cooling rate 2.5 °C/min	53.6 ± 1.2
9	Constant cooling rate 2.5 °C/min +annealing 155 °C, 10 min	62.8 ± 1.2
10	Isothermal crystallised 135 °C, 60 min	59.8 ± 6.0
11	Isothermal crystallised 135 °C, 180 min	59.3 ± 2.3

at 205 °C for 5 min and subsequently subjected to different cooling rates, crystallisation temperatures and annealing times/temperatures. As a reference, the crystallinity was determined by dsc using $H_0 = 148$ J/g [37] as the heat of fusion for the crystal. From the measured heat of fusion, H, the crystallinity was calculated as:

$$\chi^c = \frac{H}{H_0}\frac{\rho^a}{\rho^c}\left[1 - \left(1 - \frac{\rho^a}{\rho^c}\right)\right] \quad (1)$$

where $\rho^a = 0.85$ g/cm^3, $\rho^c = 0.936$ g/cm^3 are densities of the amorphous (a) and crystalline (c) state. Details of sample preparation and crystallinity (χ^c) are given in Table 2.

The analysis of the 808–840 cm^{-1} spectral region indicates a three-phase structure consisting of a crystalline phase related to the intensity of the 808 cm^{-1} band, an isomeric defect phase consisting of helical chains and related to the intensity of the 840 cm^{-1} band and a melt-like amorphous phase related to the intensity of the 830 cm^{-1} band. For a three-phase structure, a general relation between the scattering intensities can be written as

$$C_a\frac{I_{808}}{I_{ref}} + C_b\frac{I_{840}}{I_{ref}} + C_c\frac{I_{830}}{I_{ref}} = 1 \quad (2)$$

where subscript a refers to the amorphous melt-like phase, b refers to the defect phase and c refers to the crystal phase. C_a, C_b, C_c are calibration constants and I_{ref} is a reference intensity. The reference intensity is used to correlate for changes in scattering intensity not related to crystallinity. Appropriate reference peaks are peaks that are unaffected by chain conformation and crystallisation. It was found that the intensity sum $\bar{I} = I_{808} + I_{830} + I_{840}$ is independent of crystallinity within the observed range of crystallinities, Fig. 8.

Using this intensity sum as a reference intensity is equivalent to $C_a = C_b = C_c$. The fraction of the three phases is then determined as:

$$\chi^a = I_{830}/\bar{I} \qquad \chi^b = I_{840}/\bar{I} \qquad \chi^a = I_{808}/\bar{I}$$

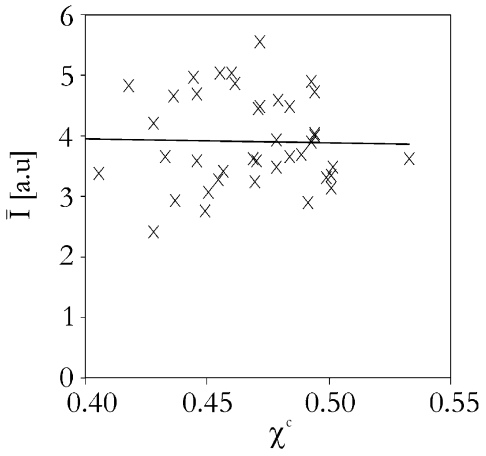

Fig. 8. Variation of $\bar{I} = I_{808} + I_{830} + I_{840}$ with crystallinity (dsc). Solid line represents a linear least-squares data regression.

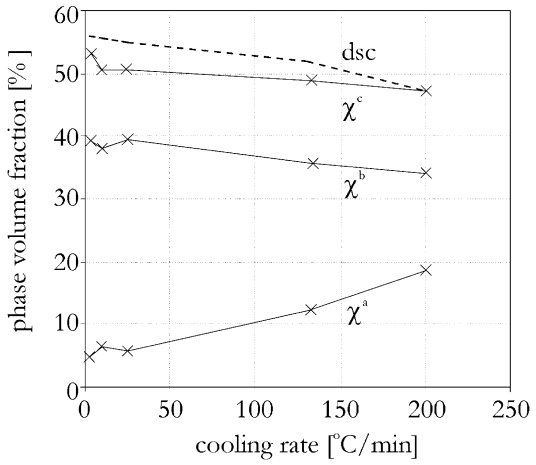

Fig. 9. Influence of cooling rate.

Table 3 shows the calculated volume fractions of the phases a, b, c. Results are compared to crystallinity determined by dsc. A close correlation between χ^{c}_{Raman} and χ^{c}_{dsc} is seen $\chi^{c,Raman} \approx 0.93\chi^{c,dsc}$.

Fig. 9 shows the variation of the three phases a, b, c with cooling rate. The correlation between Raman and dsc is evident. Increasing the cooling rate results in a decrease in the crystalline phase c. Simultaneously there is a significant increase of the melt-like amorphous phase a. This is explained by the kinetics of chain conformation and crystallisation. The variation of the defect phase b appears to follow the crystalline phase ($\chi^{b} \approx 0.83\chi^{c}$) which indicates that the defect phase is associated with crystals.

Fig. 10 shows the effect of annealing time on the variation of χ^{a} and χ^{c} of an initially quenched sample annealed at 155 °C.

When a sample is quenched, regular chains capable of forming a helical structure may appear in the amorphous phase as time has not allowed the low energy equilibrium conformation to be achieved. During annealing, time and temperature allows rearrangement of these chains to form helices and local regions of order. The remaining chains within phase a are the atactic, irregular chains which cannot form helices due to the random positioning of side-groups. These observations support the assumption of a three-phase structure Fig. 11.

Two models have been proposed to explain the presence of a third phase in association with the lamella morphology. Takayanagi [38] suggested the presence of defect regions within the crystal region. Experimental studies by Michler [39] using TEM on stained LDPE have shown that crystallites are composed of mosaic blocks of finite lateral width in the (100) and (010) crystallographic directions. Another explanation is the presence of an amorphous–crystal interphase as suggested by Flory and Yoon [40].

The proposed three-phase structure is supported by other spectroscopic studies (Raman, Nuclear Magnetic Resonance) on different polymers [15–18]. Using solid-state high resolution ^{13}C NMR spectroscopy, Saito et al. [19] observed a three-phase morphology in i-PP composed of extended 3_1 helical chains in crystal regions, helical chains in a disordered phase and chains in non-helical conformation. The conclusion of a three-phase structure was

Table 3
Calculated fractions of phases using Raman spectroscopy compared to crystallinity determined by dsc (sample numbers refer to Table 2)

Sample	χ^{c} (dsc)	χ^{a}	χ^{b}	χ^{c}
1	47.1 ± 0.8	18.7 ± 7.0	34.1 ± 7.8	47.2 ± 7.0
2	48.9 ± 6.2	9.7 ± 6.1	34.0 ± 5.6	56.3 ± 1.0
3	60.1 ± 4.3	5.5 ± 0.7	37.2 ± 1.1	57.3 ± 0.5
4	60.7 ± 2.5	6.8 ± 1.3	36.0 ± 1.2	57.2 ± 0.4
5	48.8 ± 2.7	12.3 ± 1.0	35.7 ± 1.2	52.0 ± 0.8
6	50.4 ± 1.5	5.7 ± 0.9	39.5 ± 0.8	54.8 ± 1.2
7	50.6 ± 1.0	6.3 ± 0.9	38.2 ± 1.1	55.5 ± 1.4
8	53.6 ± 1.2	4.7 ± 0.9	39.4 ± 1.2	55.9 ± 1.5
9	62.8 ± 1.2	4.7 ± 2.4	38.8 ± 2.4	56.5 ± 152
10	59.8 ± 6.0	4.3 ± 1.6	40.0 ± 0.8	55.8 ± 0.8
11	59.3 ± 2.3	3.6 ± 1.1	40.7 ± 1.0	55.7 ± 1.3

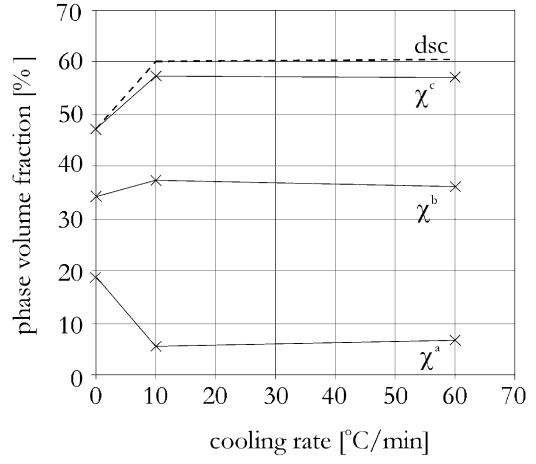

Fig. 10. Influence of annealing time at 155 °C for an initially quenched sample.

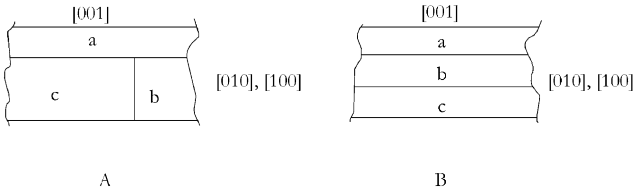

Fig. 11. Schematic models explaining the presence of a third, disordered phase (b) associated with lamellae morphology. [001] is chain direction. (A) Crystal defect region, (B) Amorphous–crystal interphase.

furthermore confirmed by density measurements which gave unrealistically high values of crystallinity, indicating an intermediate non-crystalline phase of higher density than the amorphous phase. Similar observations have been made on polyethylene using Raman spectroscopy [16–18].

4. Conclusions

The relation between Raman scattering and microstructure of isotactic polypropylene has been studied. The Raman spectrum of i-PP is mainly sensitive to the conformational state of the polymer chain. From the observation of correlation splitting three different conformational states were identified. Chains in regular helical conformation present in crystals and related to the intensity of the 808 cm^{-1} band, chains in helical conformation with defects in the *tg* conformation related to the intensity of the 840 cm^{-1} band and atactic chains in non-helical conformation related to the intensity of the 830 cm^{-1} band. From integrated intensities a quantitative relation between Raman scattering intensity and crystallinity was derived. Results were compared to dsc using as heat of fusion for the crystal 148 J/g and a good correlation was found. Experimental results show that the distribution of chains in the different conformations to some extent is determined by thermal history. With increasing cooling rate, there is a decrease in crystallinity and simultaneously a significant increase of chains in non-helical conformation. During annealing time and temperature allows part of these chains to form helices and local regions of order. This results in an increase in crystallinity and a decrease in the melt-like amorphous phase.

References

[1] Popli R, Mandelkern L. J Polym Sci Polym Phys 1987;25:441.
[2] Halpin JC, Kardos JL. J Appl Phys 1972;43:2235.
[3] Boyd RH. Polym Engng Sci 1979;19:1010.
[4] Boyd RH. J Polym Sci Polym Phys 1983;21:493.
[5] Mandelkern L. Crystallization of polymers. New York: McGraw-Hill, 1964.
[6] Mandelkern L. Polym J 1985;17:337.
[7] Negahban M, Wineman AS. Int J Engng Sci 1992;30:953.
[8] Wortmann FJ, Schulz KV. Polymer 1996;37:819.
[9] Boyd RH. Polymer 1985;26:323.
[10] Boyd RH. Macromolecules 1984;17:903.
[11] Varga J. In: Karger-Kocsis J, editor. Polypropylene: structure, blends and composites. London: Chapman & Hall, 1995. p. 56.
[12] Janeschitz-Kriegl H, Fleischmann E, Geymayer W. In: Karger-Kocsis J, editor. Polypropylene: structure, blends and composites. London: Chapman & Hall, 1995. p. 295.
[13] Eder M, Wlochowicz A. Polymer 1983;24:1593.
[14] Nakamura K, Katayama K, Amano T. J Appl Polym Sci 1973;17:1031.
[15] Boukenter A, Achibat T, Duval E, Lorentz G, Beautemps. J Polym Commun 1991;32:258.
[16] Strobl GR. The physics of polymers—concepts for understanding their structures and behaviour. Berlin: Springer, 1996.
[17] Strobl GR, Hagedorn W. J Polym Sci Polym Phys 1978;16:1181.
[18] Mutter R, Stille W, Strobl G. J Polym Sci Polym Phys 1993;31: 99.
[19] Saito S, Moteki Y, Nakagawa M, Horii F, Kitamura R. Macromolecules 1990;23:3256.
[20] Hendra PJ, Vile J, Willis HA, Zichy V. Polymer 1984;25:785.
[21] Keresztury G, Foldes E. Polym Test 1990;9:329.
[22] Everall N, Taylor P, Chalmers JM, MacKerron D, Ferwerda R, van der Maas JH. Polymer 1994;35:3184.
[23] Williams KPJ, Everall NJ. J Raman Spectrosc 1995;26:427.
[24] Stuart BH. Vibrat Spectrosc 1996;10:79.
[25] Jones CH, Wesley IJ. Spectrochim Acta 1991;47A:1293.
[26] Louden JD. Polym Commun 1986;27:82.
[27] Lehnert RJ, Hendra PJ, Everall N. Polymer 1995;36:2473.
[28] Bower DI, Maddams WF. The vibrational spectroscopy of polymers. Cambridge: Cambridge University Press, 1992.
[29] Massetti G, Cabassi F, Zerbi G. Polymer 1980;21:143.
[30] Zerbi G, Gussoni M, Ciampelli F. Spectrochim Acta 1967;23A: 301.
[31] Tadokoro H, Kobayashi M, Ukita M, Yasufuku K, Murahashi S. J Chem Phys 1965;42:1432.
[32] Snyder RG, Schachtschneider JH. Spectrochim Acta 1964;20: 853.
[33] Chalmers JM, Edwards HGM, Lees JS, Long DA, Mackenzie MW, Willis HA. J Raman Spectrosc 1991;22:613.
[34] Ozawa T. Polymer 1971;12:150.
[35] Fraser GV, Hendra PJ, Watson DS, Gall MJ, Willis HA, Cudby MEA. Spectrochim Acta 1973;29A:1525.
[36] Ize-Iyamu MI. Mater Res Bull 1983;18:225.
[37] Monasse B, Haudin JM. Colloid Polym Sci 1985;263:822.
[38] Takayanagi M. In: Lee EH, Copley AL, editors. Fourth International Congress on Rheology Part 1. New York: Interscience, 1965. p. 161.
[39] Michler GH. Kunststoff-mikromechanik. Carl-Hanser, 1992.
[40] Flory PJ, Yoon DY. Nature 1978;272:226.